Atmos. Chem. Phys. Discuss., 15, 10709–10738, 2015
www.atmos-chem-phys-discuss.net/15/10709/2015/
doi:10.5194/acpd-15-10709-2015
© Author(s) 2015. CC Attribution 3.0 License.

Atmospheric Chemistry and Physics Discussions

This discussion paper is/has been under review for the journal Atmospheric Chemistry and Physics (ACP). Please refer to the corresponding final paper in ACP if available.

Parameterizations for convective transport in various cloud-topped boundary layers

M. Sikma[1,2] **and H. G. Ouwersloot**[1]

[1]Max Planck Institute for Chemistry, Mainz, Germany
[2]Meteorology and Air Quality Section, Wageningen University, Wageningen, the Netherlands

Received: 3 March 2015 – Accepted: 28 March 2015 – Published: 14 April 2015

Correspondence to: M. Sikma (martin.sikma@wur.nl)

Published by Copernicus Publications on behalf of the European Geosciences Union.

Abstract

We investigate the representation of convective transport of atmospheric compounds that can be applied in large-scale models. We focus on three key parameterizations that, when combined, express this transport: the area fraction of transporting clouds, the upward velocity in the cloud cores and the chemical concentrations at the cloud base. The first two parameterizations combined represent the mass flux by clouds.

To investigate the key parameterizations under a wide range of conditions, we use Large-Eddy Simulation model data for 10 meteorological situations, characterized by either shallow cumulus or stratocumulus clouds. In the analysis of the area fraction of clouds, we (i) simplify the independent variable used for the parameterization, Q_1, by considering the variability in moisture rather than in the saturation deficit. We show that there is an unambiguous dependence of the area fraction of clouds on the simplified Q_1, and update the parameters in the parameterization to account for this simplification. We (ii) further demonstrate that the independent variable has to be evaluated locally to capture cloud presence. Furthermore, we (iii) show that the area fraction of transporting clouds is not represented by the parameterization for the total cloud area fraction, as is currently applied in large-scale models. To capture cloud transport, a novel active cloud area fraction parameterization is proposed.

Subsequently, the scaling of the upward velocity in the clouds' core by the Deardorff convective velocity scale and the parameterization for the concentration of atmospheric reactants at cloud base from literature are verified and improved by analyzing 6 SCu cases. For the latter, we additionally discuss how the parameterization is affected by wind conditions. This study contributes to a more accurate estimation of convective transport in large-scale models, which occurs there at sub-grid scale.

ACPD
15, 10709–10738, 2015

1 Introduction

Convective transport by shallow cumulus (SCu) clouds is a key process in the lower atmosphere, as it regulates the partitioning of surface fluxes (Vilà-Guerau de Arellano et al., 2014; Lohou and Patton, 2014) and the temporal evolution of chemical reactants (Vilà-Guerau de Arellano et al., 2005; Ouwersloot et al., 2013). By venting air from the atmospheric boundary layer (ABL) to the free troposphere, SCu strongly influence the ABL evolution, temperature, moisture content, and the variability of chemical species (Sorooshian et al., 2007; van Stratum et al., 2014). Besides their local effects, SCu contribute strongly to the spread in the estimation of climate sensitivities by affecting both longwave (greenhouse warming) and shortwave (reflective cooling) radiation (Boucher et al., 2013). This makes it essential to represent SCu and their effects accurately in atmospheric chemistry, climate and weather prediction models. However, due to the relatively coarse resolution of these models (~ 50–200 km), SCu (~ 1 km) need to be treated as a sub-grid phenomena and are therefore required to be parameterized.

Convective transport can be parameterized in large-scale models by using a convective adjustment scheme (e.g. Betts, 1986), an eddy-diffusion scheme (e.g. Tiedtke et al., 1988) or the mass flux approach (e.g. Bretherton et al., 2003). In this study, we mainly focus on the latter. The mass flux approach is based on the mass continuity equation, where the mass flux is defined as the difference between the lateral entrainment and detrainment rate. By analyzing 10 numerical experiments performed by Large-Eddy Simulations (LES), we investigate three key parameterizations that can be used to represent mass transport in large-scale models, namely: the area fraction of clouds, the upward velocity in the cloud cores and the concentrations at the cloud base. The latter is also applicable when a convective adjustment or eddy-diffusion scheme is employed.

As the initiation of SCu formation depends on surface forcings and the thermodynamic state of the ABL, we discriminate between two situations: (i) the marine ABL, and (ii) the continental ABL. Since the formation of SCu in the marine ABL is character-

ACPD
15, 10709–10738, 2015

ized by almost constant surface forcings, resulting in steady-state conditions, this situation has been extensively studied (e.g., Neggers et al., 2004; de Rooy and Siebesma, 2008; Suselj et al., 2013). The marine steady-state SCu case used in this study is the Barbados Oceanographic and Meteorological Experiment (BOMEX; Holland and Rasmusson, 1973). On the other hand, the continental ABL is affected by a diurnal cycle in surface forcings. The large variation in surface forcings during day drive the initiation of SCu formation, therefore impacting the dynamical structures in the ABL (Horn et al., 2015). As this situation is harder to study and therefore less investigated, four continental campaigns are selected, ranging from the mid-latitudes to the tropics, to serve as inspiration for the LES numerical experiments: the Tropical Forest and Fire Emissions Experiment (TROFFEE; Karl et al., 2007), the Gulf of Mexico Atmospheric Composition and Climate Study (GoMACCS; Jiang et al., 2008), the Small Cumulus Microphysics Study (SCMS; Neggers et al., 2003) and the Atmospheric Radiation Measurements (ARM; Brown et al., 2002).

In this work, we simplify the statistical cloud area fraction parameterization as described by Cuijpers and Bechtold (1995, hereafter CB95) by considering the variability in moisture rather than the saturation deficit. In contradiction to simplifications proposed in literature (e.g. Chaboureau and Bechtold, 2002; Neggers et al., 2006), we developed a general formulation that shows an unambiguous dependency of the cloud area fraction on the independent variable, Q_1, for a wide range of thermodynamic conditions. For this, we perform 10 distinct numerical simulations, where we first focus on deriving a consistent representation for the total SCu cover. Furthermore, the assumption made by Neggers et al. (2006, hereafter NG06), entailing that the cloud area fraction parameterization can be used for the representation of the area fraction of active clouds, was recently shown not to be valid for a tropical (TROFFEE) case (Sikma et al., 2014). Here, we build on this finding by proposing a novel parameterization for the area fraction of active clouds, which is appropriate for convective transport. Subsequently, extending the work of Ouwersloot et al. (2013) and van Stratum et al. (2014), we present improvements on the scaling of the vertical convective velocity. As a result, we are able

ACPD
15, 10709–10738, 2015

to accurately describe the mass flux in SCu clouds. We finalize by showing that the parameterization of chemical species concentrations at cloud base of Ouwersloot et al. (2013) can be used under a wide range of conditions, although dynamical segregation slightly influences the results. Our findings can be used in large-scale models to represent sub-grid scale convective transport, or in conceptual models to investigate SCu interactions (e.g., Vilà-Guerau de Arellano et al., 2012; van Stratum et al., 2014). Furthermore, as the the vertical velocity and cloud cover are essential to calculate cloud micro-physics and radiation properly (Arakawa, 2004), our results will enhance the representations of these in global models.

As shown by Ouwersloot et al. (2011), the chemical variability in clear sky conditions is affected by ABL dynamics, creating regions of high- and low concentrations, thereby modifying the mean reactivity. Since SCu impact the dynamical structures in the ABL (Horn et al., 2015), it will enhance this segregation of species (Kim et al., 2004). As below the SCu, the concentrations of chemical species differ more from cloud-layer concentrations than the mean concentrations in the ABL (Ouwersloot et al., 2013).

The next section introduces the theory of mass flux and is followed by the descriptions of the model and numerical experiments. In the results, we first explore the effects of cloud venting on the temporal evolution of SCu. This is followed by parameterizations of the area fraction of SCu venting and a scaling of the vertical convective velocity. We finalize with a validation and adjustment of the parameterization for the concentrations of chemical species at cloud base. While doing so, we discuss the role of dynamical segregation in the ABL.

2 Methodology

2.1 Cloud types and cloud distinction

To increase the representation of SCu and its effects in large-scale models, parameterizations are developed. As not all clouds transport ABL air to the free troposphere,

ACPD
15, 10709–10738, 2015

it is necessary to discriminate between different cloud types for convective transport predictions. Since forced clouds are related to air parcels that reach the lifting condensation level, but are buoyantly too weak to reach the level of free convection, no net mass transport occurs by these clouds. Clouds that reach the level of free convection are marked as active clouds, since the release of latent heat increases the buoyancy of the cloud, thereby enhancing cloud growth. These active clouds transport mass, which affects the underlying ABL. When these active clouds decouple from the ABL, they lose their supply of energy and become passive clouds that do not contribute to the mass transfer (Stull, 1985; Siebesma et al., 2003).

The part of the domain in which convective transport occurs, is quantified by the area fraction of clouds, which is defined at each level independently (Siebesma et al., 2003; Ouwersloot et al., 2013). Note that we cannot use cloud cover, as this property is not locally determined but based on the vertically integrated liquid water path. Furthermore, we distinguish in the remaining of the paper between all clouds and cloud cores, i.e. active clouds, with subscript $_{\mathrm{c}}$ and $_{\mathrm{cc}}$, respectively. As a result, we can distinguish four indicators for cloud presence, namely: cloud cover (c_{c}), cloud core cover (c_{cc}), area fraction of clouds (a_{c}) and area fraction of cloud cores (a_{cc}).

2.2 Mass flux parameterization

Mass transport can be approximated as the mass flux (M) multiplied with the spatial difference in the concentrations of chemical species at cloud base (ϕ) (Betts, 1973):

$$\overline{w'\phi'} = M\left(\phi_{\mathrm{cc}} - \overline{\phi}(z_{\mathrm{b}})\right), \tag{1}$$

where ϕ_{cc} indicates the value in the cloud core, and $\overline{\phi}(z_{\mathrm{b}})$ indicates the domain averaged value at cloud base.

The kinematic mass flux, M, is defined by the area fraction of cloud cores (a_{cc}), the difference between the cloud core vertical velocity (w_{cc}) and the domain averaged

ACPD
15, 10709–10738, 2015

vertical velocity at cloud base ($\overline{w}(z_b)$) (Betts, 1973), through

$$M = a_{cc}(w_{cc} - \overline{w}(z_b)). \quad (2)$$

For models that run on a coarser grid resolution than the width of a cloud core, the variables of Eq. (2) cannot be resolved explicitly and therefore need to be parameterized. We start by parameterizing the area fraction of cloud cores (a_{cc}). NG06 approximated a_{cc} by the total area fraction of clouds (a_c). The parameterization of a_c is developed by CB95, which uses locally taken variables depending on temperature and moisture, and is expressed by

$$a_c = 0.5 + \beta \arctan(\gamma \cdot Q_1). \quad (3)$$

Here the constant $\beta = 0.36$ and $\gamma = 1.55$ represent a fit through the LES results of CB95. Q_1 is calculated as

$$Q_1 = \frac{\overline{s}}{\sigma_s}. \quad (4)$$

Here, s denotes the saturation deficit and σ_s indicates the SD of s. Lenderink and Siebesma (2000) assumed for simplicity that Q_1 can be represented as

$$Q_2 = \frac{q_t - q_s}{\sigma_q}, \quad (5)$$

where q_t and q_s are, respectively, the total and saturation specific humidity, and σ_q is the spatial SD of the specific humidity. Based on this work, NG06 applied this expression for a_{cc}, while the Q_2 is replaced by Q_3, which is further simplified to be applicable in a mixed-layer slab model, according to

$$Q_3 = \frac{\langle q_t \rangle - q_s|_h}{\sigma_q|_h}. \quad (6)$$

ACPD
15, 10709–10738, 2015

Here, $\langle q_t \rangle$ is the total specific humidity averaged over the mixed layer and $q_s|_h$ and $\sigma_q|_h$ represents the respective values at the mixed-layer top. Although these adapted variables indeed coincidentally converted the expression for a_c to a reasonable prediction for a_{cc} for the case evaluated by NG06, we demonstrate in Sect. 3.2 that this is not valid for all thermodynamic and dynamic conditions and that a different formulation should be applied.

As shown by Neggers et al. (2004), the cloud core vertical velocity can be scaled with the Deardorff convective velocity scale (w_*) (Deardorff, 1970). Building on this work, Ouwersloot et al. (2013) and van Stratum et al. (2014) showed for several SCu cases that the inclusion of a prefactor improved this scaling:

$$w_{cc} \approx 0.84\, w_* \,, \tag{7}$$

which will be further verified in this study. Furthermore, Ouwersloot et al. (2013) showed that the concentrations of chemical species at the base of the active clouds can be parameterized as:

$$\phi_{cc} - \overline{\phi}(z_b) \approx -1.23 \left(\overline{\phi}(z_b) - \langle \phi \rangle \right) \,. \tag{8}$$

2.3 LES model

The numerical model used in this study is DALES 4.0. This version contains several improvements over version 3.2 (Heus et al., 2010), including additional elements (e.g. new landsurface submodels Vilà-Guerau de Arellano et al., 2014) and the introduction of an anelastic approximation for density changes with height (Boing et al., 2014). In DALES, most (∼ 90 %) of the turbulent processes are solved explicitly in a convective ABL when run on a grid resolution of 100 m or less. As a result, only parameterizations for the smaller scale turbulent structures are needed, which makes it an adequate tool to use in our study. With the use of the Boussinesq approximation, the filtered Navier–Stokes equation is solved (Heus et al., 2010). Furthermore, DALES consists of no-slip

ACPD
15, 10709–10738, 2015

boundary conditions at the bottom and periodic boundary conditions at the sides. At the top of the domain, a sponge layer is located which damps fluctuations caused by e.g. convection waves.

2.4 Numerical experiments

In all cases, the horizontal grid resolution is set to 50 m × 50 m, which covers an area of 12 km × 12 km. A larger domain or increase in grid resolution proved not to be of significance. The vertical resolution and extent are case dependent and are listed in Table 1. The direction of the wind is always set in the x direction (u component), but differences are present in the velocities (Table 1). Also the case dependent surface kinematic heat and moisture fluxes are prescribed. Furthermore, the ABL top is defined at the height where the gradient of the virtual potential temperature (θ_v) exceeds 50 % of the maximum gradient in the vertical profile of θ_v (Ouwersloot et al., 2011).

Ten numerical experiments are run to simulate a range of SCu and stratocumulus cases. Regarding the SCu, 5 situations (TROFFEE, GoMACCS, SCMS, ARM, BOMEX) are selected. Additionally, TROFFEE+ and SCMS− consider an adapted wind velocity compared to the original TROFFEE and SCMS cases, respectively. The $\mathrm{SCMS_{cold}}$ case represents an adaptation on SCMS, where the initial vertical profile of θ is lowered by 2 K. This is done to represent a transition from stratocumulus to shallow cumulus, as discussed in Sect. 3.2. Regarding the stratocumulus, 2 situations (ATEX and DYCOMS-II) are analyzed.

To investigate the diurnal impact of SCu convection, the SCu simulations start in the early morning and are based on daytime convective conditions. Depending on the geophysical location, the UV radiation is calculated as a function of time. The chemical mechanism applied in the SCu cases is identical as described in Ouwersloot et al. (2013) and contains 20 reactant species and three passive tracers. The latter are an emitted tracer (INERT; emission of 1 ppb m s^{-1}), an inert species that is initially only present in the ABL (BLS) and an inert species that is initially present in the free tropo-

ACPD
15, 10709–10738, 2015

sphere (FTS). To ensure that the reactions are fully resolved, the time step is forced to a maximum of 1 s. For all cases, the data is stored at a 1 min interval.

The stratocumulus experiments are solely performed to include representative data for the upper regime of the total cloud area fraction parameterization. Therefore, no chemical scheme is applied.

3 Results and discussion

3.1 Temporal evolution of shallow cumulus

The temporal evolution of the total and active cloud area fraction is presented in Fig. 1. The cases TROFFEE and ARM are clearly affected by a different partitioning in sensible and latent heat fluxes, caused by the diurnal cycle in incoming solar radiation. This demonstrates that the initiation of SCu formation is dependent on the surface forcing. As a result, the SCu start to develop from mid-morning and diminish in the late afternoon. The GoMACCS and SCMS cases show different dynamics compared to TROFFEE or ARM, as SCu start to develop in the early morning (06:30 and 07:00 LT, respectively). This can be explained by a high relative humidity in the initial profiles at the start of the day, therefore favoring cloud formation (not shown). The reason for these high values can be found in the geophysical location of these cases, which are close to the ocean, even though they are classified as continental cases. In contrast to the continental numerical experiments, the BOMEX case is characterized by an almost constant surface forcing over the ocean and is therefore classified as a marine steady-state case. In the first half an hour, moisture and heat is building up in the ABL, which causes the sudden formation of SCu around 05:30 LT. After 08:00 LT, the transport of energy is proportional to the supply of energy from the surface fluxes, so the temporal evolution of the area fraction of clouds and cores is in steady-state.

As is visible in Fig. 1, for all continental SCu cases a time lag of one hour is present in the initiation of a_{cc} compared to a_c. This can be explained by forced clouds, which

ACPD
15, 10709–10738, 2015

are dominant during the first hour. This is also visible in Fig. 2a, where the ratio between a_c and a_{cc} is shown. By focusing on the forced phase, it is visible that the area fraction of clouds increases during time, but that almost no active clouds are present. It is interesting to note that the dynamics in the BOMEX case are not comparable with the other cases, since it does not start in this forced phase, as mentioned earlier. In the next phase, the transition phase, the amount of clouds remains roughly equal, but the forced clouds are replaced by active clouds. During this process, the a_{cc} increases fast, indicating that the threshold for active SCu growth is overcome. In the end of the transition phase, cloud venting affects the sub-cloud layer structures by redistributing the thermals (Horn et al., 2015). As this transport of energy out of the sub-cloud layer affects the thermal structures, the amount of forced clouds decreases, due to a decrease in the amount of thermals that reach the cloud layer. Since the a_{cc} is not significantly affected by this process, the area fraction of active clouds relatively increases. This process is clearly visible in the ARM and GoMACCS case (Fig. 1). When the transport of energy is proportional to the increase in energy by the surface fluxes, we identify this period as the active phase. During the active phase, the ratio between a_c and a_{cc} is roughly constant ($a_c = 2.12\,a_{cc}$), while both gradually decrease in time. In the final phase, the dissolving phase, the number of active clouds reduces rapidly due to the diminished surface forcings, so that the clouds become decoupled from the boundary-layer thermals and active clouds are transformed into passive clouds. As such, the ratio between passive and active clouds increases (see Fig. 2a).

As we are mainly interested in mass transport by SCu, we select for further analysis our data such that we capture the time period where SCu transport is dominant. In Fig. 2b, it is visible that during the active phase the ratio between a_c and a_{cc} is not dependent on the atmospheric conditions which differ between the numerical experiments. An increase in surface forcing directly translates into an increase in cloud venting, as the mass transfer and surface fluxes are tightly coupled. An increase in surface fluxes would cause both a_c and a_{cc} to increase, with a_c increasing faster by a factor of 2.12 ($d = 0.93$). Here, d represents the index of agreement (Wilmott, 1981).

ACPD
15, 10709–10738, 2015

Comparing our unfiltered results with the results from van Stratum et al. (2014), we find that we have a slightly lower but similar slope of 2.35 (d = 0.89) for our unfiltered results instead of 2.46 (d = 0.77). In the remainder of this paper, we use the selected data to evaluate the parameterizations and scalings.

3.2 Parameterizing the area fraction

To asses the validity of the simplified statistical cloud area fraction parameterization (hereafter a_c-parameterization) of NG06 (Eq. 12 therein) under different thermodynamic conditions, ten numerical experiments are run to simulate a wide range of SCu and stratocumulus cases (see Sect. 2.4). As is shown in Fig. 3a, the a_c-parameterization of NG06 is not able to consistently represent the total cloud area fraction. Furthermore, by using Q_3, no clear dependency is visible of the cloud area fraction on specific moisture conditions. An explanation for this could be found in the dependency of Q_3 (Eq. 6) to the volume of the ABL and the thickness of the transition zone, i.e. the region between cloud base and ABL. This dependency is only introduced in NG06, since Q_1 in CB95 and Q_2 are evaluated locally. Although NG06 simplified the expression for a_c with help of Lenderink and Siebesma (2000) to reproduce the occurrence of active clouds with an atmospheric mixed-layer model, we show that this simplification can introduce significant errors depending on the evaluated case. Therefore, a revision of the a_c-parameterization is needed such that the cloud area fraction can be reproduced for a wide range of atmospheric conditions. Furthermore, an independent representation of the active cloud area fraction, necessary for convective transport, is needed. In these analyses, we use the locally determined Q_2 (Eq. 5) as indicator.

To include as many different boundary-layer physics and cloud conditions between the SCu and stratocumulus cases (i.e., between $Q_2 = -2$ and 1) as possible, two transition simulations, ATEX and $\mathrm{SCMS}_{\mathrm{cold}}$, are shown. ATEX represents a case where SCu convection starts to develop, but an inversion causes the build up of moisture near the ABL top, resulting in a stratocumulus layer. Another approach is used for the $\mathrm{SCMS}_{\mathrm{cold}}$

ACPD
15, 10709–10738, 2015

simulation, where the initial vertical profiles of θ were decreased by 2 K. As a result, the relative humidity is close to 100 % near ABL top in the morning, thereby creating a stratocumulus layer. When the surface fluxes start to increase, the stratocumulus layer breaks and convection starts to occur. As is visible in Fig. 3b, a typical SCu situation is present in the late afternoon which is comparable with the other SCu cases and is captured by the revised a_c-parameterization. As is shown in Fig. 3b, using the proper index variable, Q_2, results in a well-defined dependence of cloud area fraction. Furthermore, using this approach we can deduce an accurate parameterization for a_c for all numerical experiments. By using a least square fitting method, we find

$$a_c = 0.5 + 0.34 \arctan(1.85 Q_2 + 2.33). \quad (9)$$

In ATEX and $SCMS_{cold}$, both the SCu and stratocumulus regimes are generally captured well by Eq. (9), while only the transition between this regime remains troublesome.

As mentioned before, a_{cc} cannot be parameterized by the expression for a_c. This is confirmed by the $a_c = 2.12\, a_{cc}$ relation of Fig. 2. In Fig. 4, we show that a separate parameterization is needed for a_{cc}. Inspired by Eq. (7), we derive

$$a_{cc} = 0.292\, Q_2^{-2}. \quad (10)$$

Next to a_{cc}, we display the a_c data (shaded) in Fig. 4, together with its parameterization, in order to demonstrate that a_c and a_{cc} can be well-represented independently, but that these representations are not similar. As such, using the prediction of a_c for a_{cc} will lead to wrong predictions of the active cloud area fraction. Global models that use the parameterization of CB95 or Chaboureau and Bechtold (2002), e.g. GEM (Belair et al., 2004), FGCM-0 (Fushan et al., 2005), or CanAM4 (von Salzen et al., 2013), overestimate the mass transport. This finding is consistent with the diagnosed overestimation of boundary-layer clouds in a single-column model (SCM) found for a tropical case (Suselj et al., 2013). Furthermore, as explained earlier, the simplification of NG06 for use in an atmospheric mixed-layer model introduces inconsistencies depending on

ACPD
15, 10709–10738, 2015

the evaluated case. Using Eqs. (9) and (10) removes this dependency. Therefore, it is important to use the novel parameterization of Eq. (10) to increase the accuracy of in-cloud transport and associated feedbacks. Note that in large-scale models the local SD of moisture is needed to diagnose Q_2, which can be represented using the formulations of Tompkins (2002).

3.3 Scaling of convective transport

As the cloud core vertical velocity, w_{cc}, is the final component of the mass flux formulation (Eq. 2), we evaluate the scaling of Neggers et al. (2004) for various atmospheric conditions to complete the mass flux parameterization. Neggers et al. (2004) showed that the w_{cc} can be scaled with the Deardorff convective velocity scale (w_*). Building on this work, Ouwersloot et al. (2013) and van Stratum et al. (2014) found that a prefactor of 0.84 improved this scaling. Their analysis was based on four SCu cases, where no filtering was applied on the data to distinguish between active SCu and forced/passive SCu. Therefore, the presence of forced and passive clouds disturbs the scaling of w_{cc}. As a result, their value of the scaling is lower due to the weaker vertical velocities related to forced clouds. By only taking the active phase into account, we find the following relation (Fig. 5):

$$w_{cc} = 0.91\, w_*, \tag{11}$$

with $d = 0.90$. The high index of agreement shows that this relation is not affected much by different boundary-layer dynamics and structures. However, as is visible in Fig. 5, the TROFFEE case is less well represented by the scaling. If we apply a fit through TROFFEE data alone, we find a scaling factor of 0.845 ($d = 0.74$), which is comparable to the result of Ouwersloot et al. (2013) who found 0.84 ($d = 0.94$). The deviation of this case compared to other cases could be explained by a relative deep ABL depth (~ 2 km). Combined with strong surface forcings, the w_* increases strongly, while the w_{cc} is not significantly affected. This results in a lower scaling constant.

ACPD
15, 10709–10738, 2015

3.4 Parameterizing reactant transport

In this section we focus on the final component of the expression for convective transport of atmospheric compounds (Eq. 1), namely the concentration of chemical species at cloud base ($(\phi_{cc} - \overline{\phi}(z_b))$). The parameterization is proposed by Ouwersloot et al. (2013) who showed that the concentrations of chemical species at the base of active SCu can be predicted by Eq. (8) for a tropical case (TROFFEE). However, they stress that their parameterization can be influenced by ABL dynamics. Therefore, we test the parameterization for all continental SCu cases. The relation is illustrated for four chemical species (i.e., INERT, BLS, isoprene and CO) in Fig. 6. In total, the least squares regression through the concentrations of all 24 evaluated chemical species yields for our continental SCu data:

$$\phi_{cc} - \overline{\phi}(z_b) \approx -1.18 \left(\overline{\phi}(z_b) - \langle\phi\rangle\right) . \quad (12)$$

For all relations, the amount of data yields a d of 1.00.

Comparing these results with Ouwersloot et al. (2013) shows that our constant is slightly less negative than their −1.23. Since we use the least squares method to find the optimum scaling constant, it implies that compounds with the largest differences between $(\phi(z_b) - \langle\phi\rangle)$ affect the scaling constant the most. As is shown in Fig. 6, this means that INERT has a dominating influence. Focusing on this compound (inset), we see that wind tends to increase the differences between species in the cloud core compared to their average at cloud base, while for a free convection situation the opposite is visible. As a result, the closure constant of Eq. (12) shifts slightly. In this case, we find a slope of −1.17 in case of wind and a slope of −1.19 in case of free convection (not shown). We identify for the INERT species that dynamical segregation is occurring in the ABL, as shown in Fig. 7 and discussed by Ouwersloot et al. (2013). Rising motions in the ABL transport high concentration of the emitted species upwards, while lower concentration of INERT are found in the downward motions. Therefore, higher concentrations of species are transported towards the free troposphere by cloud vent-

ACPD
15, 10709–10738, 2015

ing as would be expected compared to a well-mixed situation. As a result, the chemical parameterizations and scalings are effected. As is shown in Fig. 7, wind affects the distance and upward velocities in the thermals, resulting in less, but wider thermals in our domain. Furthermore, the vertical transport of species is slower (max. $3.5\,\mathrm{m\,s^{-1}}$) compared to a free convection situation (max. $5.0\,\mathrm{m\,s^{-1}}$) where the thermals are more narrow. As an effect, the transport of chemical species to the cloud layer is less in the wind case, resulting in a smaller difference between ϕ_{cc} and $\overline{\phi}(z_b)$, which decreases the magnitude of the scaling constant of Eq. (12). Next to affecting the convective transport, dynamical segregation also modifies the mean reactivity in the ABL, as was shown by Ouwersloot et al. (2011) for clear sky conditions and Kim et al. (2004) in SCu situations.

4 Conclusions

In this paper, the representation of sub-grid convective transport of atmospheric compounds in large-scale models is investigated. We focused on three key parameterizations that express this transport, namely: the area fraction of clouds, the upward velocity in the cloud cores and the concentrations at cloud base. The parameterizations are investigated under a wide range of conditions with the use of Large-Eddy Simulation (LES) model data from seven boundary-layer cloud cases, ranging from SCu (partly cloud cover) to stratocumulus (totally overcast). Next to the seven standard boundary-layer cloud cases, three additional cases are simulated that are slightly adapted to provide additional information needed for deriving the parameterizations.

We found that the simplified statistical cloud area fraction parameterization, and the combined variables it uses as input, are influenced by the structure of the atmospheric boundary layer (ABL). Therefore, the parameterization was not applicable to a wide range of conditions. We simplified and updated this parameterization by considering the variability in moisture rather than the saturation deficit, and show that this parameterization has to be evaluated locally to properly capture cloud presence. Furthermore,

ACPD
15, 10709–10738, 2015

we demonstrate that the parameterization for the total cloud area fraction cannot be used to represent the area fraction of active clouds, as is currently assumed in literature and applied in large-scale models. To capture this cloud transport, a novel parameterization is proposed.

Moreover, we evaluated the scaling of the cloud core vertical velocity with the Deardorff convective velocity scale by using 6 continental representative SCu cases. It was found that the previously published relation holds, but that a higher closure constant improves this relation. Combining the parameterizations for the area fraction of active clouds and the cloud core vertical velocity, we are able to accurately represent the mass flux induced by SCu clouds.

To finalize our analysis, the parameterization of reactant concentrations at the base of active clouds is investigated for the 6 continental SCu cases. We found a minor spread in the derived closure constants for the parameterization, depending on whether a background wind is present or not, which can be explained by the affected dynamical segregation of chemical species in the ABL. However, this spread is small and a general derived closure constant can be applied for parameterizations in large-scale models. In total, we validated and updated three robust parameterizations that can be used in large-scale models to represent sub-grid scale convective transport of chemical species.

Acknowledgements. The authors would like to thank Jordi Vilà-Guerau de Arellano for the insightful discussions and comments. The numerical simulations were performed with the supercomputer facilities at SURFsara and sponsored by the project NCF-NWO SH-060-13.

The article processing charges for this open-access publication were covered by the Max Planck Society.

ACPD
15, 10709–10738, 2015

References

Arakawa, A.: The Cumulus Parameterization Problem: past, present and future, J. Climate, 17, 2493–2525, doi:10.1175/1520-0442(2004)017<2493:RATCPP>2.0.CO;2, 2004. 10713

Belair, S., Mailhot, J., Girard, C., and Vaillancourt, P.: Boundary-layer and shallow cumulus clouds in a medium-range forecast of a large-scale weather system, Mon. Weather Rev., 133, 1938–1960, doi:10.1175/MWR2958.1, 2004. 10721

Betts, A. K.: Non-precipitating cumulus convection and its parameterization, Q. J. Roy. Meteor. Soc., 99, 178–196, doi:10.1002/qj.49709941915, 1973. 10714, 10715

Betts, A. K.: A new convective adjustment scheme, Part I: Observational and theoretical basis, Q. J. Roy. Meteor. Soc., 112, 677–691, doi:10.1002/qj.49711247307, 1986. 10711

Boing, S. J., Jonker, H. J. J., Nawara, W., and Siebesma, A. P.: On the deceiving aspects of mixing diagrams of deep cumulus convection, J. Atmos. Sci., 71, 56–68, doi:10.1175/JAS-D-13-0127.1, 2014. 10716

Boucher, O., Randall, D., Artaxo, P., Bretherton, C., Feingold, G., Forster, P., Kerminen, V.-M., Kondo, Y., Liao, H., Lohmann, U., Rasch, P., Satheesh, S. K., Sherwood, S., Stevens, B., and Zhang, X. Y.: Clouds and aerosols, in: Climate Change 2013: The Physical Science Basis, Contribution of Working Group I to the Fifth Assessment Report of the Intergovernmental Panel on Climate Change, Cambridge University Press, Cambridge, UK, New York, NY, USA, 2013. 10711

Bretherton, C. S., McCaa, J. R., and Grenier, H.: A new parameterization for shallow cumulus convection and its application to marine subtropical cloud-topped boundary layers, Part I: Description and 1D results, Mon. Weather Rev., 132, 864–882, doi:10.1175/1520-0493(2004)132<0864:ANPFSC>2.0.CO;2, 2003. 10711

Brown, A. R., Cederwall, R. T., Chlond, A., Duynkerke, P. G., Golaz, J. C., Khairoutdinov, M., Lewellen, D. C., Lock, A. P., Macvean, M. K., Moeng, C. H., Neggers, R. A. J., Siebesma, A. P., and Stevens, B.: Large-eddy simulation of the diurnal cycle of shallow cumulus convection over land, Q. J. Roy. Meteor. Soc., 128, 1075–1093, doi:10.1256/003590002320373210, 2002. 10712, 10731

Chaboureau, J. and Bechtold, P.: A simple cloud parameterization derived from cloud resolving model data: diagnostic and prognostic applications, J. Atmos. Sci., 59, 2362–2372, 2002. 10712, 10721

ACPD
15, 10709–10738, 2015

Cuijpers, J. W. M. and Bechtold, P.: A simple parameterization of cloud water related variables for use in boundary layer models, J. Atmos. Sci., 52, 2486–2490, doi:10.1175/1520-0469(1995)052<2486:ASPOCW>2.0.CO;2, 1995. 10712

de Rooy, W. C. and Siebesma, A. P.: A simple parameterization for detrainment in shallow cumulus, Mon. Weather Rev., 136, 560–576, doi:10.1175/2007MWR2201.1, 2008. 10712

Deardorff, J. W.: Convective velocity and temperature scales for the unstable planetary boundary layer and for Rayleigh convection, J. Am. Meteorol. Soc., 27, 1211–1213, doi:10.1175/1520-0469(1970)027<1211:CVATSF>2.0.CO;2, 1970. 10716

Fushan, D., Rucong, Y., Xuehong, Z., Yongqiang, Y., and Jianglong, L.: Impacts of an improved low-level cloud scheme on the eastern Pacific ITCZ-Cold Tongue Complex, Adv. Atmos. Sci., 22, 559–574, doi:10.1007/BF02918488, 2005. 10721

Heus, T., van Heerwaarden, C. C., Jonker, H. J. J., Pier Siebesma, A., Axelsen, S., van den Dries, K., Geoffroy, O., Moene, A. F., Pino, D., de Roode, S. R., and Vilà-Guerau de Arellano, J.: Formulation of the Dutch Atmospheric Large-Eddy Simulation (DALES) and overview of its applications, Geosci. Model Dev., 3, 415–444, doi:10.5194/gmd-3-415-2010, 2010. 10716

Holland, J. Z. and Rasmusson, E. M.: Measurements of the atmospheric mass, energy, and momentum budgets over a 500-Kilometer square of tropical ocean, Mon. Weather Rev., 101, 45–57, doi:10.1175/1520-0493(1973)101<0044:MOTAME>2.3.CO;2, 1973. 10712

Horn, G. L., Ouwersloot, H. G., Vilà-Guerau de Arellano, J., and Sikma, M.: Cloud shading effects on characteristic boundary layer length scales, Bound.-Lay. Meteor., under review, 2015. 10712, 10713, 10719

Jiang, H., Feingold, G., Jonsson, H. H., Lu, M.-L., Chuang, P. Y., Flagan, R. C., and Seinfeld, J. H.: Statistical comparison of properties of simulated and observed cumulus clouds in the vicinity of Houston during the Gulf of Mexico Atmospheric Composition and Climate Study (GoMACCS), J. Geophys. Res., 113, D13205, doi:10.1029/2007JD009304, 2008. 10712, 10731

Karl, T., Guenther, A., Yokelson, R. J., Greenberg, J., Potosnak, M., Blake, D. R., and Artaxo, P.: The tropical forest and fire emissions experiment: Emission, chemistry, and transport of biogenic volatile organic compounds in the lower atmosphere over Amazonia, J. Geophys. Res., 112, D18302, doi:10.1029/2007JD008539, 2007. 10712

ACPD
15, 10709–10738, 2015

Kim, S.-W., Barth, M. C., and Moeng, C.-H.: The effect of shallow cumulus convection on the segregation of chemical reactants, 16th Symposium on Boundary Layers and Turbulence, 67–70, Portland, 2004. 10713

Lenderink, G. and Siebesma, A. P.: Combining the mass flux approach with a statistical cloud scheme, in: Proceedings of the 14th Symposium on Boundary Layer and Turbulence, Aspen, 66–69, 2000. 10715, 10720

Lohou, F. and Patton, E.: Surface energy balance and buoyancy response to shallow cumulus shading, J. Atmos. Sci., 71, 665–682, doi:10.1175/JAS-D-13-0145.1, 2014. 10711

Neggers, R. A. J., Duynkerke, P. G., and Rodts, S. M. A.: Shallow cumulus convection: a validation of large-eddy simulation against aircraft and Landsat observations, Q. J. Roy. Meteor. Soc., 129, 2671–2696, doi:10.1256/qj.02.93, 2003. 10712, 10731

Neggers, R. A. J., Siebesma, A., Lenderink, G., and Holtslag, A.: An evaluation of mass flux closures for diurnal ccycle of shallow cumulus, Mon. Weather Rev., 132, 2525–2538, doi:10.1175/MWR2776.1, 2004. 10712, 10716, 10722

Neggers, R. A. J., Stevens, B., and Neelin, J. D.: A simple equilibrium model for shallow-cumulus-topped mixed layers, Theor. Comput. Fluid Dyn., 20, 305–322, doi:10.1007/s00162-006-0030-1, 2006. 10712, 10734

Ouwersloot, H. G., Vilà-Guerau de Arellano, J., van Heerwaarden, C. C., Ganzeveld, L. N., Krol, M. C., and Lelieveld, J.: On the segregation of chemical species in a clear boundary layer over heterogeneous land surfaces, Atmos. Chem. Phys., 11, 10681–10704, doi:10.5194/acp-11-10681-2011, 2011. 10713, 10717

Ouwersloot, H. G., Vilà-Guerau de Arellano, J., van Stratum, B. J. H., Krol, M. C., and Lelieveld, J.: Quantifying the transport of subcloud layer reactants by shallow cumulus clouds over the Amazon, J. Geophys. Res., 118, 13041–13059, doi:10.1002/2013JD020431, 2013. 10711, 10712, 10713, 10714, 10716, 10717, 10722, 10723, 10731, 10737

Siebesma, A. P., Bretherton, C. S., Brown, A., Chlond, A., Cuxart, J., Duynkerke, P. G., Jiang, H., Khairoutdinov, M., Lewellen, D., Moeng, C., Sanchez, E., Stevens, B., and Stevens, D. E.: A large eddy simulation intercomparison study of shallow cumulus convection, J. Atmos. Sci., 60, 1201–1219, doi:10.1175/1520-0469(2003)60<1201:ALESIS>2.0.CO;2, 2003. 10714, 10731

Sikma, M., Vilà-Guerau de Arellano, J., and Ouwersloot, H. G.: An elementary shallow cumulus parameterization for tropical boundary layers, in: Proceedings of the 5th Student Research Conference, November, Delft, 2014. 10712

ACPD
15, 10709–10738, 2015

Sorooshian, A., Lu, M.-L., Brechtel, F. J., Jonsson, H., Feingold, G., Flagan, R. C., and Seinfeld, J. H.: On the source of organic acid aerosol layers above clouds, Environ. Sci. Technol., 41, 4647–4654, doi:10.1021/es0630442, 2007. 10711

Stevens, B., Ackerman, A. S., Albrecht, B. A., Brown, A. R., Chlond, A., Cuxart, J., Duynkerke, P. G., Lewellen, D. C., Macvean, M. K., Neggers, R. A. J., Sanchez, E., Siebesma, A. P., and Stevens, D. E.: Simulations of trade wind cumuli under a strong inversion, J. Atmos. Sci., 58, 1870–1891, doi:10.1175/1520-0469(2001)058<1870:SOTWCU>2.0.CO;2, 2001. 10731

Stevens, B., Moeng, C.-H., Ackerman, A. S., Bretherton, C. S., Chlond, A., de Roode, S., Edwards, J., Golaz, J. C., Jiang, H., Khairoutdinov, M., Kirkpatrick, M. P., Lewellen, D. C., Lock, A., Muller, F., Stevens, D. E., Whelan, E., and Zhu, P.: Evaluation of large-eddy simulations via observations of nocturnal marine stratocumulus, Mon. Weather Rev., 133, 1443–1462, doi:10.1175/MWR2930.1, 2005. 10731

Stull, R. B.: A fair weather cumulus cloud classification scheme for mixed layer studies, J. Clim. Appl. Meteorol., 24, 49–56, doi:10.1175/1520-0450(1985)024<0049:AFWCCC>2.0.CO;2, 1985. 10714

Suselj, K., Teixeira, J., and Chung, D.: A unified model for moist convective boundary layers based on a stochastic eddy-diffusivity/mass-flux parameterization, J. Atmos. Sci., 70, 1929–1953, doi:10.1175/JAS-D-12-0106.1, 2013. 10712, 10721

Tiedtke, M., Heckley, A., and Slingo, J.: Tropical forecasting at ECMWF: the influence of physical parametrization on the mean structure of forecasts and analyses, Q. J. Roy. Meteor. Soc., 114, 639–664, doi:10.1002/qj.49711448106, 1988. 10711

Tompkins, A. M.: A prognostic parameterization for the subgrid-scale variability of water vapor and clouds in large-scale models and its use to diagnose cloud cover, J. Atmos. Sci., 59, 1917–1942, doi:10.1175/1520-0469(2002)059<1917:APPFTS>2.0.CO;2, 2002. 10722

van Stratum, B. J. H., Vilà-Guerau de Arellano, J., van Heerwaarden, C. C., and Ouwersloot, H. G.: Subcloud-layer feedback driven by the mass flux of shallow cumulus convection over land, J. Atmos. Sci., 71, 881–895, doi:10.1175/JAS-D-13-0192.1, 2014. 10711, 10712, 10713, 10716, 10720, 10722

Vilà-Guerau de Arellano, J., Kim, S.-W., Barth, M. C., and Patton, E. G.: Transport and chemical transformations influenced by shallow cumulus over land, Atmos. Chem. Phys., 5, 3219–3231, doi:10.5194/acp-5-3219-2005, 2005. 10711

ACPD
15, 10709–10738, 2015

Vilà-Guerau de Arellano, J., van Heerwaarden, C. C., and Lelieveld, J.: Modelled suppression of boundary-layer clouds by plants in a CO_2-rich atmosphere, Nat. Geosci., 5, 701–704, doi:10.1038/NGEO1554, 2012. 10713

Vilà-Guerau de Arellano, J., Ouwersloot, H. G., Baldocchi, D., and Jacobs, C.: Shallow cumulus rooted in photosynthesis, Geophys. Res. Lett., 41, 1796–1802, doi:10.1002/2014GL059279, 2014. 10711, 10716

von Salzen, K., Scinocca, J. F., McFarlane, N. A., Li, J., Cole, J. N. S., Plummer, D., Verseghy, D., Reader, M. C., Ma, X., Lazarae, M., and Solheim, L.: The Canadian Fourth Generation Atmospheric Global Climate Model (CanAM4), Part I: Representation of physical processes, Atmos. Ocean, 51, 104–125, doi:10.1080/07055900.2012.755610, 2013. 10721

Wilmott, C. J.: On the validation of models, Phys. Geogr., 2, 184–194, 1981. 10719

ACPD
15, 10709–10738, 2015

Table 1. Experimental setup of the shallow cumulus and stratocumulus cases.

Case	Vertical resolution [m]	Vertical extent [m]	Wind u comp. [$m\,s^{-1}$]	Case type	Reference to LES case/ Comments
TROFFEE	20	5990	0.0	Continental SCu	Ouwersloot et al. (2013)
TROFFEE+	20	5990	5.0	Continental SCu	Adapted, including wind
GoMACCS	25	4988	0.0	Continental SCu	Jiang et al. (2008)
SCMS	20	3990	5.65685[a]	Continental SCu	Neggers et al. (2003)
SCMS−	20	3990	0.0	Continental SCu	Adapted, removing wind
ARM	20	4490	10.0	Continental SCu	Brown et al. (2002)
BOMEX	40	3180	−8.75[b]	Marine SCu	Siebesma et al. (2003)
$SCMS_{cold}$	20	3990	5.65685[a]	Transition case	Adapted, decrease of 2 K in θ
ATEX	20	3990	−8.0[b]	Transition case	Stevens et al. (2001)
DYCOMS-II	10	1595	3.02[b]	Marine stratocumulus	Stevens et al. (2005)

[a] Rotated wind vector which is comparable with the actual SCMS case.
[b] Height dependent wind profiles, starting at surface. A more detailed description can be found in the references.

ACPD
15, 10709–10738, 2015

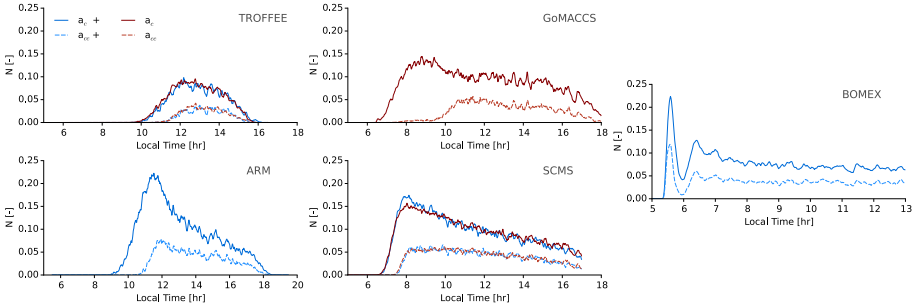

Figure 1. Temporal evolution of the domain averaged maximum area fraction (N) of clouds and cores for the SCu cases (Table 1). The blue lines denote an experiment with wind (indicated with a "+"), while the red lines indicate a free convection case.

ACPD
15, 10709–10738, 2015

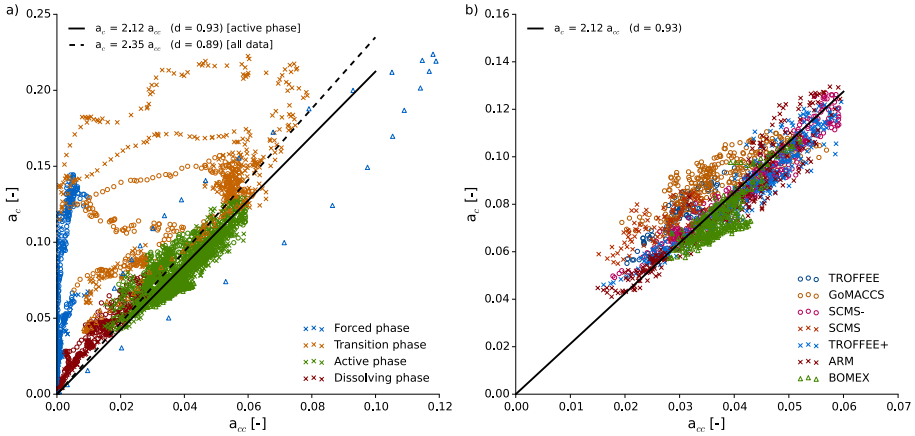

Figure 2. Scaling of the area fraction of clouds as a function of the area fraction of cloud cores. In **(a)** all data is presented, where a distinction is made between different phases of convection during day. The lines represent the best fit through the active phase and all data, forced through 0. In **(b)** the selected data is shown for each SCu case. Circles indicate free convection situations, while crosses indicate wind situations. To differentiate BOMEX from the other cases, BOMEX is marked with triangles in **(a)** and **(b)**. Furthermore, *d* represents the index of agreement.

ACPD
15, 10709–10738, 2015

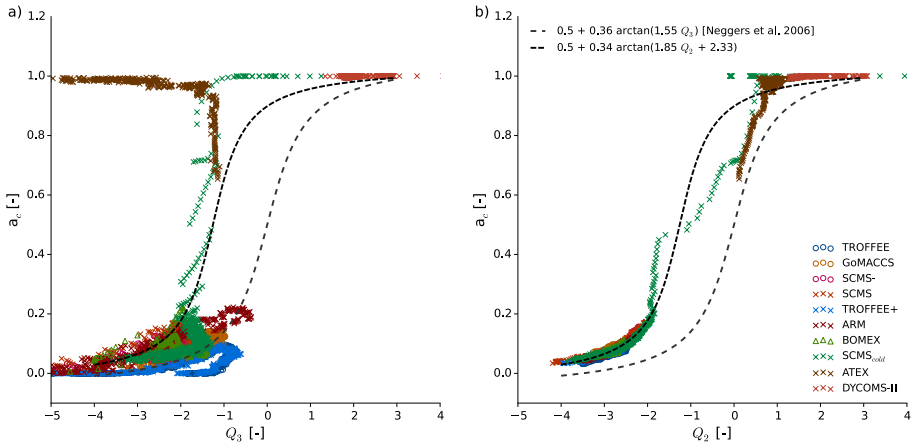

Figure 3. Area fraction of clouds as **(a)** a function of the normalized saturation deficit (Q_3; Eq. 6) as described in Neggers et al. (2006) and **(b)** as a function of the normalized saturation deficit at cloud base (Q_2; Eq. 5). Negative Q_2 and Q_3 values indicate SCu clouds, while positive values denote stratocumulus clouds. The dashed lines indicate the parameterizations based on Q_3 and Q_2.

ACPD
15, 10709–10738, 2015

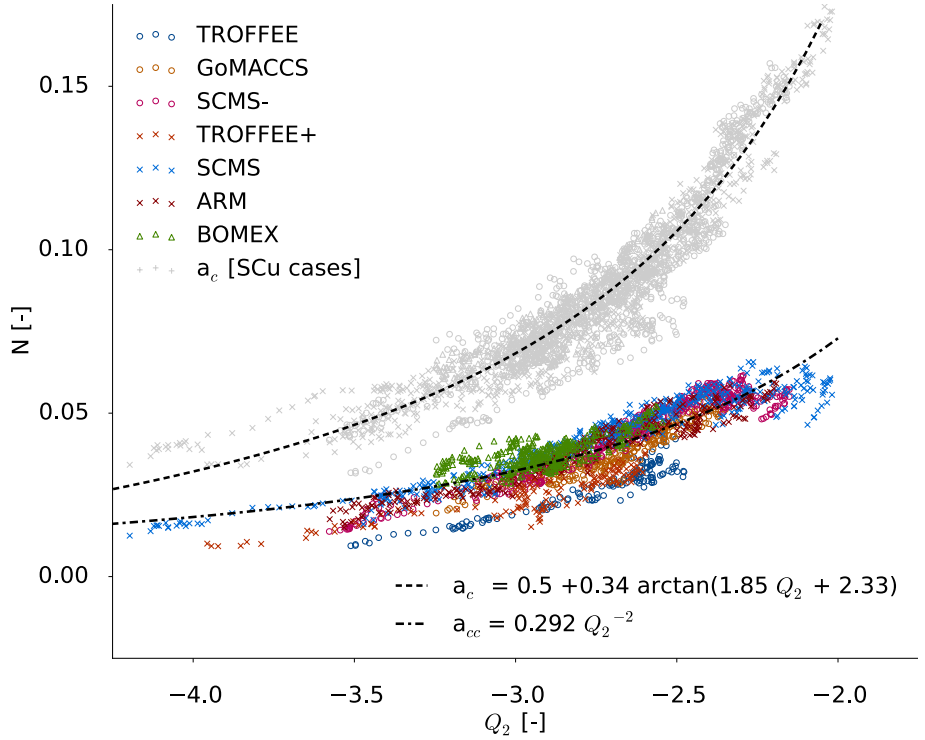

Figure 4. The area fraction of cloud cores (a_{cc}) is represented by the coloured symbols, while the a_c for all SCu cases is shown in grey. Both area fractions are shown as a function of the normalized saturation deficit at cloud base (Q_2). Crosses denote a wind situations, while circles indicate free convection situations. The lines represent the best fit parameterizations for a_c and a_{cc}.

ACPD
15, 10709–10738, 2015

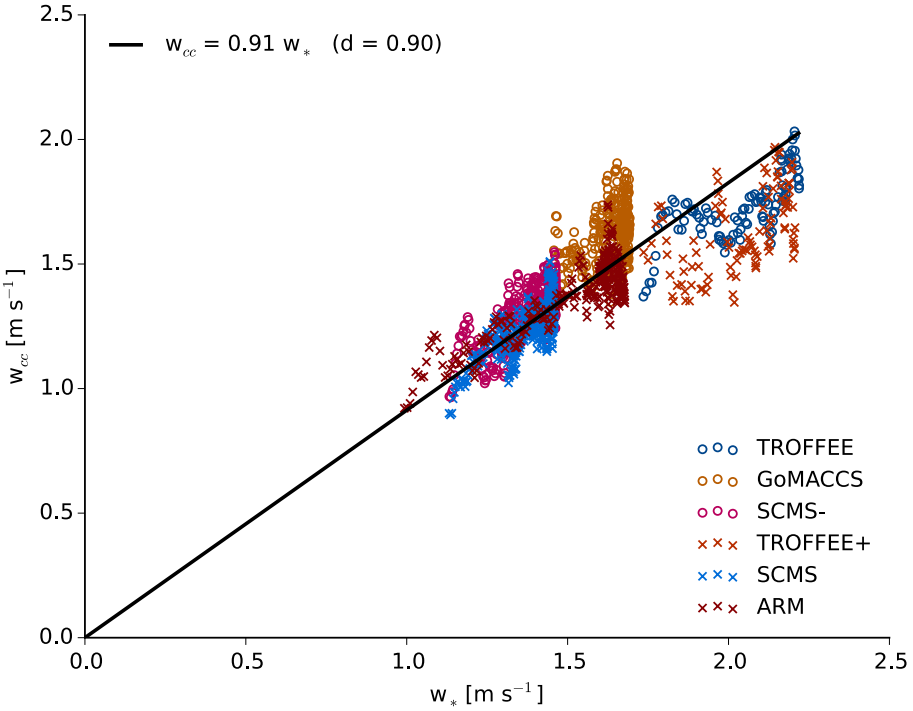

Figure 5. Scaling of the cloud core vertical velocity (w_{cc}) as a function of the Deardorff convective velocity scale (w_*). Circles represent free convecition situations, crosses indicate wind situations. The line represents a least square fit, which is forced through 0. *d* represents the index of agreement.

ACPD
15, 10709–10738, 2015

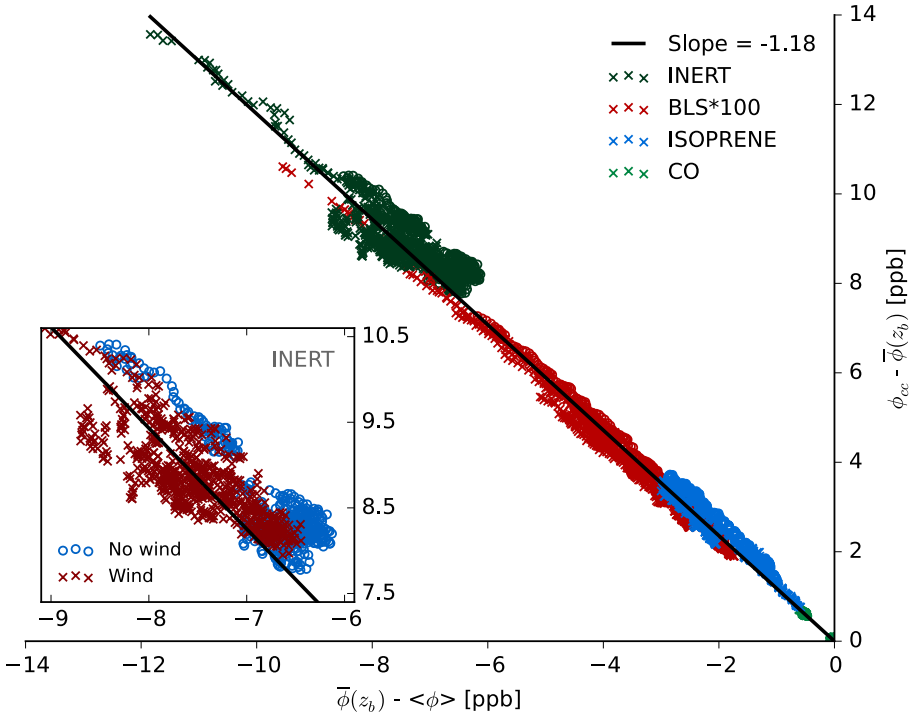

Figure 6. Parameterization for $\phi_{cc} - \overline{\phi}(z_b)$ as a function of $\overline{\phi}(z_b) - \langle\phi\rangle$ proposed by Ouwersloot et al. (2013). Here, ϕ represents the 24 transported species (note that only INERT, BLS, isoprene and CO are shown). Circles represent free convecition situations, crosses indicate wind situations. The solid line represents a least square fit trough all data, which is forced through 0. *d* represents the index of agreement. The inset shows solely the INERT species for wind and no wind experiments.

ACPD
15, 10709–10738, 2015

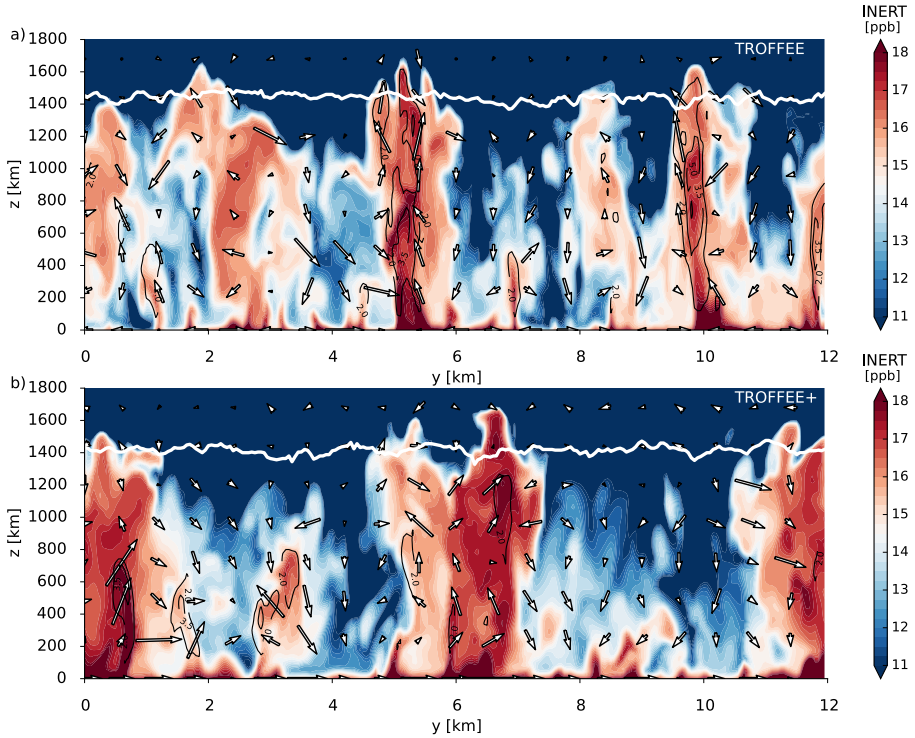

Figure 7. Vertical cross sections of INERT for the TROFFEE case for **(a)** a free convection situation and **(b)** a wind situation. The white arrows indicate wind vectors of the *v* and *w* component. In **(b)**, the mean horizontal wind is substracted from the flow to identify the vertical patterns. The white horizontal line around 1400 m denotes the ABL heigth, which is calculated using the threshold gradient method. In black, contour lines are shown for *w*, starting at a lower limit of $2\,m\,s^{-1}$ with intervals of $1.5\,m\,s^{-1}$.

ACPD
15, 10709–10738, 2015